

# 1 A Fast and Non-destructive Terahertz Dissolution Assay for Immediate Release Tablets

2 Prince Bawuah<sup>1</sup>, Daniel Markl<sup>2,3</sup>, Alice Turner<sup>2,4</sup>, Mike Evans<sup>5</sup>, Alessia Portieri<sup>5</sup>, Daniel  
3 Farrell<sup>5</sup>, Ralph Lucas<sup>6</sup>, Andrew Anderson<sup>7</sup>, Daniel J. Goodwin<sup>7</sup> and J. Axel Zeitler\*<sup>1</sup>

4 <sup>1</sup>University of Cambridge, Department of Chemical Engineering and Biotechnology, UK

5 <sup>2</sup>University of Strathclyde, Strathclyde Institute of Pharmacy and Biomedical Sciences,  
6 Glasgow, UK

7 <sup>3</sup>EPSRC Future Manufacturing Research Hub for Continuous Manufacturing and Advanced  
8 Crystallisation (CMAC), University of Strathclyde, Technology and Innovation Centre,  
9 Glasgow, UK

10 <sup>4</sup>The CMAC National Facility, The EPSRC CMAC Future Manufacturing Research Hub, The  
11 Technology and Innovation Centre, The University of Strathclyde, 99 George Street, Glasgow,  
12 G1 1RD, UK

13 <sup>5</sup>TeraView Limited, 1, Enterprise, Cambridge Research Park, CB25 9PD, Cambridge, UK

14 <sup>6</sup>Huxley Bertram Engineering Ltd, 53 Pembroke Avenue, Waterbeach, Cambridge, UK

15 <sup>7</sup>GSK, David Jack Centre, Research and Development, Park Road, Ware, Hertfordshire, UK

## 16 Abstract

17 There is a clear need for a robust process analytical technology tool that can be used for on-  
18 line/in-line prediction of dissolution and disintegration characteristics of pharmaceutical tablets  
19 during manufacture. Tablet porosity is a reliable and fundamental critical quality attribute  
20 which controls key mass transport mechanisms that govern disintegration and dissolution  
21 behaviour. A measurement protocol was developed to measure the total porosity of a large  
22 number of tablets in transmission without the need for any sample preparation. By using this  
23 fast and non-destructive terahertz spectroscopy method it is possible to predict the  
24 disintegration and dissolution of drug from a tablet in less than a second per sample without  
25 the need of a chemometric model. The validity of the terahertz porosity method was established  
26 across a range of immediate release (IR) formulations of ibuprofen and indomethacin tablets  
27 of varying geometries as well as with and without debossing. Excellent correlation was  
28 observed between the measured terahertz porosity, dissolution characteristics (time to release  
29 50% drug content) and disintegration time for all samples. These promising results and  
30 considering the robustness of the terahertz method pave the way for a fully automated at-  
31 line/on-line porosity sensor for real time release testing of IR tablets dissolution.

32

33 **Keywords:** Terahertz spectroscopy, pharmaceutical tablet, porosity, disintegration,  
34 dissolution, real time release testing, process analytical technology

## 35 1. Introduction

36 In-vitro dissolution testing has long been used in the pharmaceutical industry as the benchmark  
37 for the evaluation of the quality of pharmaceutical tablets and even though in-vitro/in-vivo

---

\* Corresponding author: Axel Zeitler

Email address: jaz22@cam.ac.uk

1 correlations are not commonly expected dissolution testing is still widely considered as an  
2 important indicator of the release rate of drug. Traditional quality control methods (dissolution,  
3 disintegration, and hardness/tensile strength) are resource intensive, time consuming and  
4 destructive and only sample a relatively small proportion of drug product either through in-  
5 process control tests or batch-testing of the end-product. The need to improve product quality  
6 whilst reducing the use of costly and destructive end-product testing methods was catalysed by  
7 the Quality-by-Design (QbD) and Process Analytical Technology (PAT) initiatives <sup>1,2</sup>. Both  
8 QbD and PAT resulted in the development and implementation of innovative methods that can  
9 monitor process parameters during pharmaceutical development and manufacturing to ensure  
10 the quality of the end product. The idea of ensuring the quality of in-process and the final  
11 product based on process data is the definition of the so-called real-time release testing (RTRT)  
12 <sup>3,4</sup>.

13 To support the development of RTRT of pharmaceutical tablets, research groups have made  
14 use of fast and non-destructive dissolution-prediction methods based on near infrared (NIR) <sup>5-</sup>  
15 <sup>8</sup> and Raman <sup>7</sup> spectroscopic techniques in combination with the use of process variables such  
16 as blender speed, feed frame speed, and compaction force followed by performing multivariate  
17 regressions (chemometric analyses) <sup>5</sup>. Other NIR methods have capitalised on the detection of  
18 strain <sup>6</sup> and chemical information of disintegrants <sup>9</sup> for predicting dissolution performance of  
19 tablets. Alternative methods that employ the use of magnetic resonance imaging techniques as  
20 well as different kinds of mathematical modelling methods to predict the dissolution of given  
21 drug substances from tablets and also to study the effect of process parameters on the  
22 dissolution profile of a drug from a tablet have been reported <sup>10-15</sup>. However, the use of the  
23 above methods to reliably predict the dissolution profiles is still challenging. This is due to the  
24 inability of these methods to directly probe and quantify the bulk physical properties of tablets,  
25 e.g. porosity, that directly govern mass transport mechanisms in a tablet during its  
26 disintegration and subsequent drug release <sup>16,17</sup>.

27 In the case of immediate release (IR) tablets, the disintegration and the drug release processes  
28 are tightly linked and the International Conference on Harmonization (ICH) Tripartite  
29 Guideline Q6A <sup>18</sup> has extensively discussed cases where disintegration testing may be  
30 employed as a substitute for dissolution testing. Studies that seek to establish correlation  
31 between the dissolution of a drug from a tablet and the overall tablet disintegration have been  
32 reported in the literature <sup>19-21</sup>. An extensive review on tablet's disintegration mechanism and  
33 measurement techniques by Markl and Zeitler further provides more insight into how tablet  
34 disintegration is a necessary requirement for release and dissolution of the drug from IR tablets  
35 and hence the need for methods that can reliably quantify the disintegration rate of tablets <sup>22</sup>.  
36 It has been established in the pharmaceutical sciences community that tablet disintegration is  
37 impacted by several factors, starting from the physical properties of the tablets (porosity,  
38 surface morphology and particle size), solvent penetration/wicking, swelling and strain  
39 recovery <sup>22-25</sup>.

40 Building on the influence of the physical properties of tablets, it is a known fact that porosity  
41 plays a major role in disintegration performance of IR tablets <sup>26</sup>. In terms of the influence of

1 porosity on the release and dissolution of drug from a tablet, Hattori and Otsuka <sup>27</sup> have  
2 reiterated that the rate at which water penetrates a tablet significantly depends on the porosity.  
3 In related studies, Delalonde and Ruiz <sup>28</sup> have shown the interplay between dissolution kinetics  
4 of drug and porosity whereas Riippi et al., <sup>29</sup> have initially reported on a promising correlation  
5 between porosity and dissolution rate of erythromycin acistrate from tablet samples in the late  
6 1990s.

7 Despite the clear observed dependence of the release and dissolution behaviour of drug on the  
8 total porosity of an IR tablet, from the regulatory point of view, the measurement of tablet  
9 porosity has not been a popular method for checking the quality of IR tablets in the industry.  
10 This may be due partly to the relatively time-consuming and destructive nature of existing  
11 conventional porosity measurement methods like mercury or helium porosimetry <sup>16,29,30</sup>. The  
12 quest to develop fast and non-destructive methods to measure the porosity therefore triggered  
13 researchers like Shah et al. <sup>7</sup> to employ NIR and Raman spectroscopy to predict the porosity of  
14 tablets. Yet, these methods typically only probe surface properties and rely on the use of  
15 chemometric models. Given the surface measurement, the results may not necessarily represent  
16 the bulk tablet property. To overcome the above limitations, terahertz time-domain  
17 spectroscopy (THz-TDS) has been developed in transmission to directly measure the porosity  
18 of tablets <sup>31-33</sup> without chemometric analysis. The terahertz porosity method has the advantage  
19 that it is fast (under a second), non-destructive, non-invasive and requires no sample  
20 preparation. A recent tutorial by Bawuah et al. <sup>34</sup> has systematically outlined the steps involved  
21 in the terahertz porosity measurement method.

22 By bearing in mind the direct influence of drug release rate of a tablet by its porosity as well  
23 as the ability to quickly and accurately measure porosity by THz-TDS, a previous work by  
24 Markl et al. <sup>17</sup> has established a strong correlation between the measured terahertz effective  
25 refractive index/porosity and the drug dissolution characteristics of IR tablets. Based on the  
26 observed promising correlation, the researchers proposed the development of a robust at-line  
27 or in-line terahertz-based sensor to monitor disintegration and hence the drug dissolution  
28 performance of tablets during manufacture <sup>17</sup>.

29 This study demonstrates the use of terahertz technology to predict the drug dissolution  
30 outcomes from directly compressed IR tablets with different levels of complexity. The validity  
31 and robustness of the terahertz-based porosity measurement method was tested by probing a  
32 wide range of samples comprised of simple placebo biconvex round tablets, complex flat-faced  
33 and biconvex tablets containing active pharmaceutical ingredients (APIs), i.e., ibuprofen or  
34 indomethacin, with and without debossing.

## 35 **2. Materials and Methods**

### 36 **2.1. Materials**

37 Two APIs, ibuprofen (BLD Pharmatech, Shanghai, China) and indomethacin (Sigma-Aldrich  
38 Company Ltd., Gillingham, UK), were each formulated as IR tablets with dose strengths of 1%  
39 w/w and 10% w/w for each respective API. The formulations for each API at both doses

1 composed of common excipients, microcrystalline cellulose (MCC) (Avicel PH-102, FMC  
 2 Europe NV, Brussels, Belgium), lactose anhydrous (Supertab21AN, DFE pharma, Goch,  
 3 Germany), croscarmellose sodium (CCS) (DuPont Nutrition, Wilmington DE, USA), and  
 4 magnesium stearate (Fisher Scientific, Fair Lawn NJ, USA). Table 1 gives the %w/w of the  
 5 components used at the two dose strengths, i.e., 1% w/w API formulations (F1) and 10% w/w  
 6 API formulations (F2). The proportion of microcrystalline cellulose and lactose anhydrous,  
 7 serving as diluents and binders, were kept constant in all formulations. Magnesium stearate  
 8 and croscarmellose sodium were added to respectively serve as a lubricant and a disintegrant.  
 9 In total, four formulations were prepared, i.e., F1-Ibup, F1-Indo, F2-Ibup and F2-Indo, where  
 10 the abbreviations Ibup and Indo indicate the two APIs ibuprofen and indomethacin,  
 11 respectively.

Materials	F1		F2	
	%w/w	Quantity (g)	%w/w	Quantity (g)
Microcrystalline cellulose	43.2	86.4	39.1	78.2
Lactose anhydrous	51.8	103.6	46.9	93.8
Croscarmellose sodium	3.0	6.0	3.0	6.0
Magnesium stearate	1.0	2.0	1.0	2.0
API (Ibuprofen/Indomethacin)	1.0	2.0	10.0	20.0
<b>Total</b>	<b>100.0</b>	<b>200.0</b>	<b>100.0</b>	<b>200.0</b>

12 **Table 1:** Material composition of the two dose strengths, F1 and F2 formulations, used in the  
 13 direct compaction of all the tablets.

## 14 2.2. Methods

### 15 2.2.1. Tablet Compaction

16 The powder formulations were blended using a Turbula T2F Mixer (Willy A. Bachofen AG,  
 17 Switzerland). During the blending step, all the materials except magnesium stearate were  
 18 continuously mixed together for 10 mins followed by the addition of the magnesium stearate  
 19 and further mixing for an extra 1 min. In all, the blending process lasted for 11 mins at a speed  
 20 of 32 rpm.

21 Five batches, i.e., based on 5 different porosity levels spanning the range of about 2 - 24%, of  
 22 biconvex round tablets were directly compressed using a compaction simulator (HB50, Huxley  
 23 Bertram Engineering Ltd, UK). The compaction simulator was configured to mimic an  
 24 industrial scale tablet press (Fette 2090) with a maximum compression speed of 60 rpm. All  
 25 the tablets were compressed at a targeted weight of 400 mg with varying thicknesses in order  
 26 to achieve the required porosity levels. Fifteen tablets per batch were compressed and each  
 27 tablet was collected and stored in a labelled plastic bag.

28 To test the robustness of the terahertz method similar (with same compression parameters)  
 29 batches of biconvex tablets with debossing “TPI” inscribed on one side were compressed from  
 30 the same formulations (see Table S1 in the supplementary information). Only debossed tablets  
 31 were used for both APIs’ F2 formulations.

1 The nominal porosity ( $f_{\text{nominal}}$ ) of the batches, as given by Eq. (1), was measured several days  
2 after the compaction, but just before the terahertz measurements were conducted, to allow for  
3 possible post-compaction mechanical relaxation of the tablets.

$$4 \quad f_{\text{nominal}} = 1 - \frac{\rho_{\text{tablet}}}{\rho_{\text{true}}}, \quad (1)$$

5 where the tablet density,  $\rho_{\text{tablet}}$ , was calculated from the weight ( $W$ ) and physical dimensions,  
6 i.e., height ( $H$ ) and diameter ( $d$ ). The true density,  $\rho_{\text{true}}$ , of the four F1 and F2 formulations was  
7 measured using a helium pycnometer (Multipycnometer MVP-1; Quantachrome Corporation,  
8 New York, NY). The height and diameter of all the tablets were measured using a micrometre  
9 (Sealey Digital External Micrometer 0 – 25 mm; Rapid Electronics Limited, Colchester, UK)  
10 and their weights were measured with an analytical balance (Fisher Scientific, Illkirch-  
11 Graffenstaden, France). Table 2 gives the batch-average of the measured physical parameters  
12 at the two dose strengths (F1 and F2) of both the ibuprofen and indomethacin biconvex tablets  
13 without debossing.

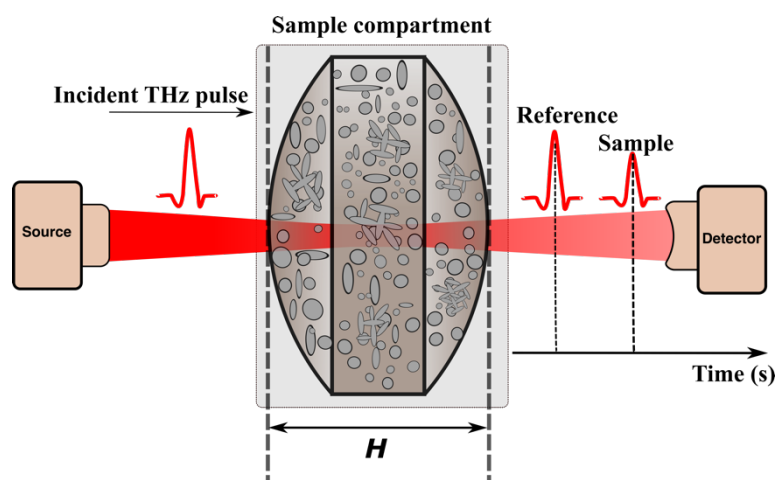
#### 14 **2.2.2. Terahertz Time-Domain Spectroscopy**

15 Terahertz time-domain measurements of all the batches were acquired using a TeraPulse 4000  
16 (TeraView Ltd., Cambridge, UK). A fast-scanning method (SpectralSeries) with overall  
17 acquisition time of  $\approx 1$  s was used. With an acquisition rate of 15 Hz, 20 waveforms were  
18 acquired and averaged. The sample compartment of the THz-TDS was continuously purged  
19 with nitrogen gas throughout the measurements to minimize the impact of water vapour on the  
20 measured THz signal. In this study using a given placebo biconvex tablets with a similar  
21 excipient composition as the current formulations, we have shown that it is possible to  
22 accurately measure the porosity of tablets by reducing the acquisition time to about one eighth  
23 of a second (0.12 s). Section 2 of the supplementary information gives detailed information  
24 about the formulation, physical dimensions, and results of the used placebo tablets.

25 A typical routine undertaken during the terahertz transmission measurements is to acquire  
26 reference measurement, i.e., conducting the measurement with an empty (nitrogen gas)  
27 compartment, followed by the sample measurements (Fig.1). The effective refractive index,  
28  $n_{\text{eff}}$ , of the tablets was measured using the frequency-domain (FD) material parameter  
29 extraction approach<sup>34</sup>. The FD method requires the conversion of the acquired time domain  
30 (TD) signals into complex FD signals via a fast Fourier transform (FFT). The frequency  
31 dependent effective refractive index of the tablets was extracted from the phase information by  
32 firstly normalising the obtained sample spectrum with the reference spectrum and secondly,  
33 going through a standard phase retrieval routine as discussed in<sup>35</sup>. Further detailed description  
34 on how to estimate the optical constants of materials using THz-TDS has been extensively  
35 reported in the literature<sup>36-40</sup>. Once the phase difference ( $\theta$ ) has been accurately determined,  
36 the effective refractive index ( $n_{\text{eff}}$ ) was estimated as

$$37 \quad n_{\text{eff}}(\nu) = \frac{c\theta}{2\pi\nu H} + 1, \quad (2)$$

1 where  $\nu$  is the frequency of the terahertz radiation,  $H$  is the tablet thickness, and  $c$  is the speed  
2 of light in vacuum. In cases where it is possible to measure the back reflection, or second echo  
3 of the terahertz pulse, the thickness of the tablets could be directly derived from the terahertz  
4 measurement itself. However, for the majority of the drug products this is unlikely to be the  
5 case given the relatively thick structures of typical tablets which would require relatively long  
6 (optical) time-delay lines in the spectrometer. In addition, even though the tablet matrix does  
7 not absorb terahertz radiation very strongly compared to other spectral ranges the absorption  
8 from the tablet may nevertheless be too high to reliably detect the second echo reflection signal  
9 after the terahertz pulse has propagated three times through the entire thickness of the tablet. It  
10 is not inconceivable that future improvements in instrumentation, for example by using very  
11 high intensity pulses of terahertz radiation, could make this possible.



12  
13 **Fig. 1.** Sample and reference terahertz pulse measurements.  $H$  indicate the thickness of the  
14 tablet.

### 15 2.2.3. Zero-Porosity Refractive Index Measurements

16 The zero-porosity refractive indices (also known as intrinsic refractive indices) of all the F1  
17 and F2 formulations, i.e., the refractive index of only the solid material of the tablets, were  
18 measured using 5 batches of flat-faced round non-debossed tablets compressed from each  
19 formulation, i.e., F1-Ibup, F1-Indo, F2-Ibup and F2-Indo. Table S5 of the supplementary  
20 information gives the detailed description of the measured parameters of the flat-faced round  
21 tablets used for the material characterisation experiments. Flat-faced tablets were used to  
22 ensure the accurate determination of the intrinsic refractive index of the formulations given the  
23 relatively simple and homogenous nature of flat-faced tablets compared to biconvex tablets.  
24 Once the accurate intrinsic refractive indices of the formulations are known, the porosity of  
25 batches of tablets with different geometries compressed from these formulations can be  
26 measured by the terahertz method.

### 27 2.2.4. Disintegration Testing

28 The disintegration testing was performed on 6 tablets per batch on the F1- and F2-based  
29 biconvex tablets without debossing (see Table 2). The performed disintegration testing  
30 complies with the requirements of the current United States Pharmacopeia (USP) chapter 701  
31 <sup>41</sup>, and the European Pharmacopeia (EP) standard 2.9.1 <sup>42</sup>, using a standard disintegration tester  
32 (DT50, SOTAX AG, Switzerland). The DT50, with a mechanical agitation rate of  $30 \pm 1$

1 strokes per minute, allows the testing of 6 tablets per test and comes with a basket that  
2 accommodates 6 tubes and 6 disks. The disks, with their conducting elements, are used to  
3 automatically detect the endpoint of the disintegration process, which reduces the variability  
4 of the measurement. Water ( $\approx 1000$  mL preheated to  $37^\circ\text{C}$ ) was used as the immersion fluid  
5 during the experiment.

### 6 **2.2.5. Dissolution Testing**

7 Samples were run by USP II paddle method using an ALS ADT8 dissolution bath coupled with  
8 an ALS SP700 UV spectrometer (Automated Lab Systems, Wokingham, Berkshire, U.K.). The  
9 ibuprofen tablets were run in pH 7.2 phosphate buffer as required by the British Pharmacopoeia  
10 <sup>43</sup> whereas the indomethacin tablets were run in pH 6.2 phosphate buffer to meet the standard  
11 requirements of United State of America Pharmacopoeia <sup>44</sup>.

12 Initially a calibration curve was produced for each drug in the relevant media. Due to the low  
13 aqueous solubility of both drugs, 1 mg/mL stock solutions were prepared in methanol before  
14 diluting with their respective buffers to produce standards of 50, 25, 10, 5 and  $2.5\ \mu\text{g mL}^{-1}$ .  
15 Both drugs were initially spectrum tested using the UV spectrometer. Ibuprofen was observed  
16 to have an absorption maximum at 222 nm and indomethacin was found to exhibit an  
17 absorption maximum at 265 nm, based on a path length of 10 mm. Analysis was carried out  
18 using the ALS software UV Win.

19  
20 A dissolution method was developed and carried out using the ALS software IDIS. Samples  
21 were run in 900 mL of buffer each with a paddle speed of 50 rpm at  $37^\circ\text{C} \pm 0.5^\circ\text{C}$ . Utilising an  
22 autosampler, all samples were taken at intervals of 80 s until the dissolution profile was found  
23 to level off and remain constant. As the system is a closed loop there was no need for  
24 replacement media to be utilised. The dissolution testing was performed on the F1 and F2  
25 biconvex tablets without debossing (see Tables 2). Additional information regarding the  
26 dissolution experiments is given in section 4 of the supplementary information. We used 6  
27 tablets of each batch and the averaged results for the whole dissolution profile for each batch  
28 is shown in Fig. S5 of the supplementary information.

### 29 **2.2.6. Hardness Testing**

30 For the hardness testing, sets of biconvex tablets with the same process conditions as those of  
31 Table 2 were again produced from the same F1 and F2 formulations (see Table 3). These sets  
32 were without debossing and all the tablets were crushed using a Kraemer Elektronik Hardness  
33 Tester HC 6.2 (Kraemer Elektronik GmbH, Darmstadt, Germany). The obtained tablet  
34 hardness, i.e. the maximum diametral crushing force,  $F$ , of the batches as given in Table 3 was  
35 further converted to tensile strength,  $\sigma_T$ , according the expression developed by Pitt et al. for  
36 cylindrical convex-faced compacts <sup>45,46</sup> shown as

$$37 \quad \sigma_T = \frac{10F}{\pi d^2 \left( 2.84 \frac{H}{d} - 0.126 \frac{H}{L} + 3.15 \frac{L}{d} + 0.01 \right)}, \quad (3)$$

1 where  $d$ ,  $H$  and  $L$  are the diameter, thickness, and cylindrical length of the biconvex tablets  
 2 respectively.

### 3 3. Results and Discussion

4 The batch-average of the measured physical parameters of both the ibuprofen and  
 5 indomethacin biconvex tablets used for the disintegration and dissolution experiments are  
 6 given Table 2. The averaged parameters for similar sets of tablets used for the hardness testing  
 7 experiments are also given by Table 3. All tablets in the Tables 2 & 3 were compressed from  
 8 the same F1 and F2 formulations respectively.

Formulation	Batch	$H$ (mm)	$d$ (mm)	$W$ (mg)	$f_{\text{nominal}}$ (%)
F1-Ibup	B1	4.572	10.055	399.6±4.0	2.85±0.13
	B2	4.712	10.056	400.6±4.0	6.35±0.54
	B3	4.932	10.074	394.5±3.0	13.28±0.56
	B4	5.204	10.090	398.5±3.0	18.41±0.61
	B5	5.418	10.098	402.3±4.0	21.77±0.62
F1-Indo	B1	4.582	10.044	403.7±2.0	1.60±0.13
	B2	4.733	10.047	402.6±2.0	5.95±0.29
	B3	4.959	10.055	403.7±2.0	11.30±0.33
	B4	5.229	10.066	405.1±1.0	16.93±0.12
	B5	5.459	10.073	404.4±1.0	21.53±0.24
F2-Ibup	B1	4.678	10.057	396.5±3.0	3.50±0.20
	B2	4.878	10.061	397.2±2.0	8.48±0.21
	B3	5.060	10.067	396.9±2.0	12.80±0.33
	B4	5.276	10.083	396.7±2.0	17.54±0.48
	B5	5.528	10.089	409.0±3.0	19.90±0.57
F2-Indo	B1	4.570	10.047	395.6±2.0	2.32±0.15
	B2	4.828	10.048	405.5±2.0	6.80±0.27
	B3	4.961	10.052	397.8±5.0	11.76±0.77
	B4	5.199	10.064	396.3±3.0	17.32±0.51
	B5	5.403	10.069	397.7±2.0	21.01±0.36

9 **Table 2:** The measured averaged parameters of the five batches of biconvex tablets compressed  
 10 from the F1 and F2 formulations. Each batch composed of 15 tablets without debossing. The  
 11 measured true densities of the formulations were,  $\rho_{\text{true}}$  (F1-Ibup) = 1.485 g cm<sup>-3</sup>,  $\rho_{\text{true}}$  (F1-Indo)  
 12 = 1.479 g cm<sup>-3</sup>,  $\rho_{\text{true}}$  (F2-Ibup) = 1.439 g cm<sup>-3</sup>, and  $\rho_{\text{true}}$  (F2-Indo) = 1.465 g cm<sup>-3</sup>.

Formulation	Batch	$H$ (mm)	$d$ (mm)	$W$ (mg)	$f_{\text{nominal}}$ (%)	Hardness (N)
F1-Ibup	B1	4.665	10.073	403.9±2.0	4.58±0.15	170.9±4.1
	B2	4.731	10.076	402.0±3.0	6.78±0.32	143.0±4.8
	B3	4.970	10.089	404.2±4.0	12.20±0.65	93.1±5.7
	B4	5.217	10.107	399.1±4.0	18.74±0.68	52.4±4.5
	B5	5.427	10.123	396.6±2.0	23.35±0.48	30.0±2.3
F1-Indo	B1	4.580	10.058	398.2±3.0	3.08±0.21	276.6±8.6
	B2	4.763	10.063	404.4±3.0	6.54±0.47	209.0±8.1
	B3	4.968	10.075	398.1±3.0	13.01±0.54	125.0±6.4

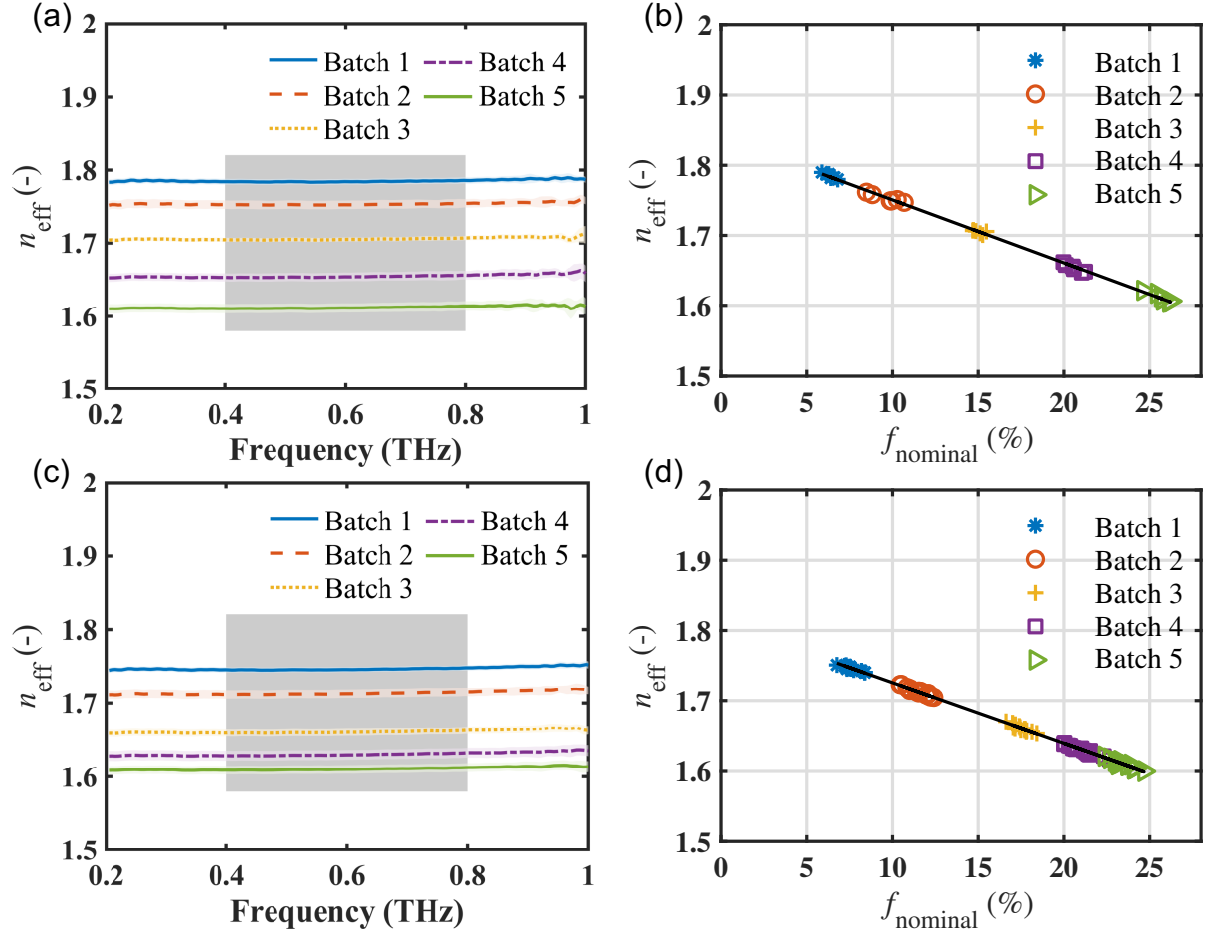
	B4	5.235	10.086	400.1±2.0	18.33±0.45	77.6±3.9
	B5	5.476	10.094	401.9±3.0	22.58±0.47	52.2±3.0
F2-Ibup	B1	4.685	10.065	396.0±3.0	3.92±0.20	185.7±6.6
	B2	4.869	10.069	403.1±4.0	7.00±0.45	139.8±6.7
	B3	5.034	10.079	399.2±3.0	11.88±0.58	90.9±6.0
	B4	5.309	10.104	395.6±4.0	18.66±0.68	45.1±3.8
	B5	5.520	10.112	396.6±6.0	22.45±1.06	31.3±3.7
F2-Indo	B1	4.639	10.059	403.7±2.0	2.43±0.18	247.9±8.5
	B2	4.797	10.068	399.9±2.0	7.59±0.25	143.3±4.0
	B3	5.009	10.076	399.4±3.0	12.80±0.54	89.7±5.0
	B4	5.275	10.091	403.1±4.0	17.77±0.71	53.6±5.1
	B5	5.517	10.110	394.9±4.0	24.05±0.76	24.8±2.8

1 **Table 3:** The measured averaged parameters of the five batches of biconvex tablets compressed  
2 from the F1 and F2 formulations and used for the hardness experiments. 10 non-debossed  
3 biconvex tablets were compressed per batch.

#### 4 **3.1. Zero-Porosity Refractive Index Measurements**

5 In this study, prior to the measurement of the zero-porosity refractive index of the formulation,  
6 the effective refractive index spectra of the flat-faced tablets were extracted via the FD data  
7 analysis (Fig. 2). A single-valued effective refractive index was obtained for each tablet by  
8 selecting and averaging the refractive indices within a range of frequency (see the shaded  
9 portion in Figs. 2 (a) and (c)). The selected effective refractive indices (Figs. 2 (b) and (d))  
10 were then used for measuring the zero-porosity refractive index of the formulation via the  
11 anisotropic Bruggeman model <sup>31</sup>. The values of the measured zero-porosity refractive index,  
12  $n_{\text{solid}}$ , for the four different formulations are listed in Table 4.

13 The criteria for choosing the frequency(ies) from which the effective refractive indices were  
14 selected strongly depended on the instrument characteristics as well as the dispersion properties  
15 of the materials involved as we have discussed previously <sup>34</sup>.



1  
2 **Fig. 2.** Effective refractive index of the F1-Ibup (a, b) and F2-Ibup (c, d) flat-faced round  
3 tablets. The frequency range, where the refractive index was selected, is indicated by the shaded  
4 portions in (a) and (c). (b) and (c) show an excellent linear correlation between the effective  
5 refractive index and the nominal porosity with a coefficient of correlation of  $R^2 = 0.999$ , root  
6 mean square error of RMSE = 0.0024 and  $R^2 = 0.999$ , RMSE = 0.0017 for the F1-Ibup and F2-  
7 Ibup, respectively. Similar results obtained for the F1-Indo and F2-Indo flat-faced round tablets  
8 are shown in Fig. S3 in the supplementary information.

9 The effective refractive index values used for the measurement of the zero-porosity refractive  
10 index of the formulation as well as terahertz porosity measurements for all the batches were  
11 selected and averaged using the frequency range of 0.4 – 0.8 THz. This range, as shown by the  
12 rectangular shaded portion in Fig. 2, possessed negligible dispersion for all the batches.  
13 Additionally, the selected frequency range lies within the range of 0.3 - 0.9 THz, where the  
14 current THz instrument exhibits its maximum signal-to-noise ratio.

Formulation	$n_{\text{solid}}$
F1-Ibup	1.839
F1-Indo	1.846
F2-Ibup	1.810
F2-Indo	1.824

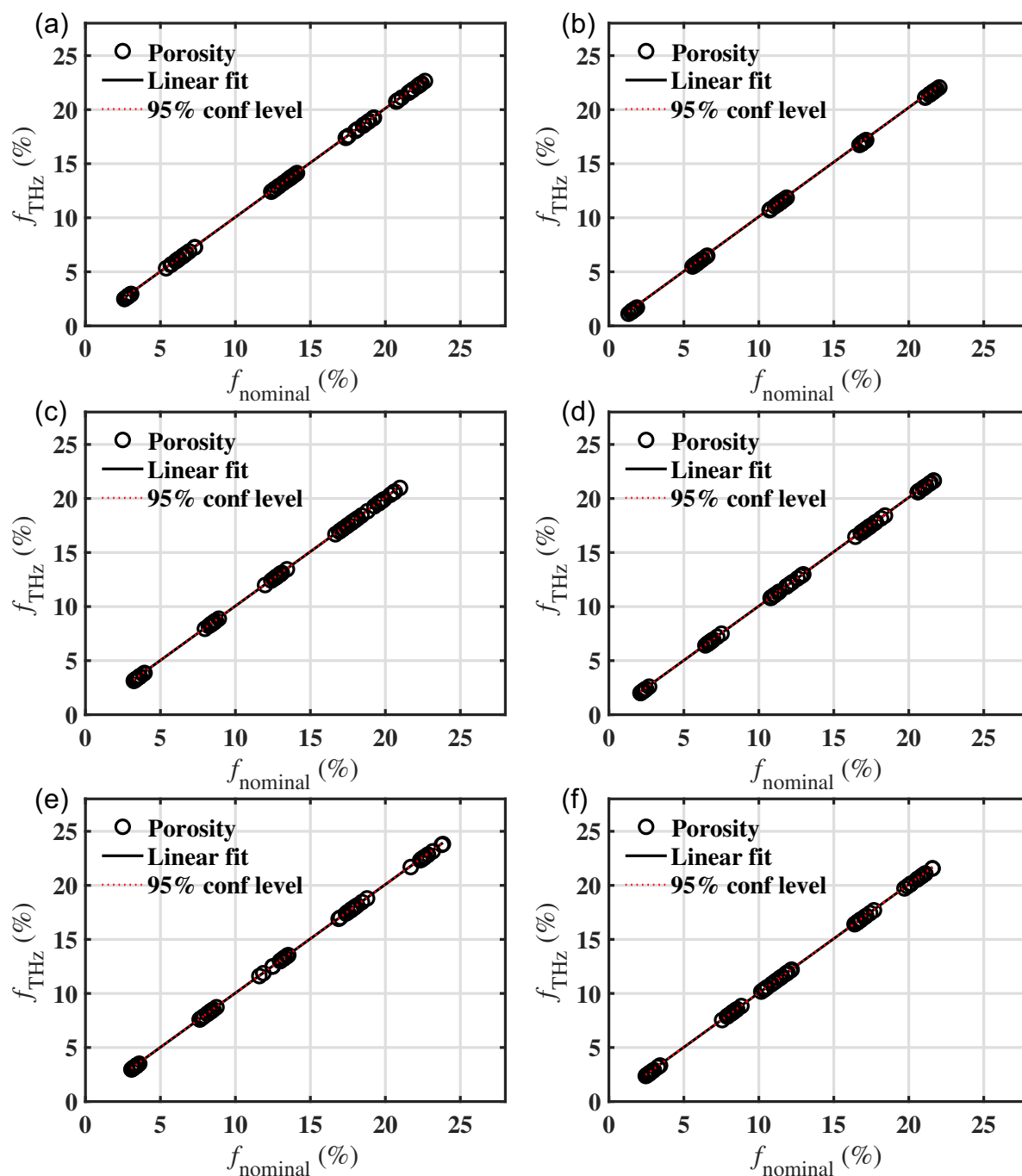
15 **Table 4:** The measured zero-porosity refractive indices,  $n_{\text{solid}}$ , of the four formulations.

### 3.2. Terahertz Porosity Measurements

The terahertz porosity,  $f_{\text{THz}}$ , of the biconvex tablets was determined using the AB-EMA<sup>31</sup> with the extracted effective refractive indices (see Fig. S1 in the supplementary information) and the zero-porosity refractive indices of the formulations obtained from the flat-faced tablets (Table 4). Despite the use of relatively high terahertz absorbing APIs, Fig. 3 shows excellent linear correlations between the measured terahertz porosity,  $f_{\text{THz}}$ , and the nominal porosity,  $f_{\text{nominal}}$ . The promising results obtained for the debossed tablets (Fig. 3 (e) & (f)) in comparison with non-debossed counterparts (Fig. 3 (c) & (d)) demonstrates the robustness of the terahertz porosity measurement method. In other words, the presence of debossing, as typically found on most commercial tablets, has negligible impact on the measured terahertz porosity.

To further buttress the robustness of the terahertz porosity measurement method, excellent correlations between  $f_{\text{THz}}$  and  $f_{\text{nominal}}$  were obtained for the flat-faced tablets (see Fig. S4 in the supplementary information), the placebo tablets (Fig. S2 in the supplementary information) and the non-debossed biconvex tablets (Table 3 and in Fig. S6 in the supplementary information). Based on the excellent results of both flat-faced and biconvex tablets in conjunction with the relatively long Rayleigh range of the used terahertz beam as we have extensively discussed in<sup>34</sup>, we can infer that curvature, lensing effect and thickness of the tablets have negligible impact on the measured porosity.

Adding to the above merits, the results obtained from the placebo tablets (Fig. S2 in the supplementary information) have proven the possibility of even scaling the acquisition time down to one eighth of a second. An acquisition time of 0.12 s means we can realise an at-line/on-line terahertz sensor that can measure up to 30,000 tablets per hour.

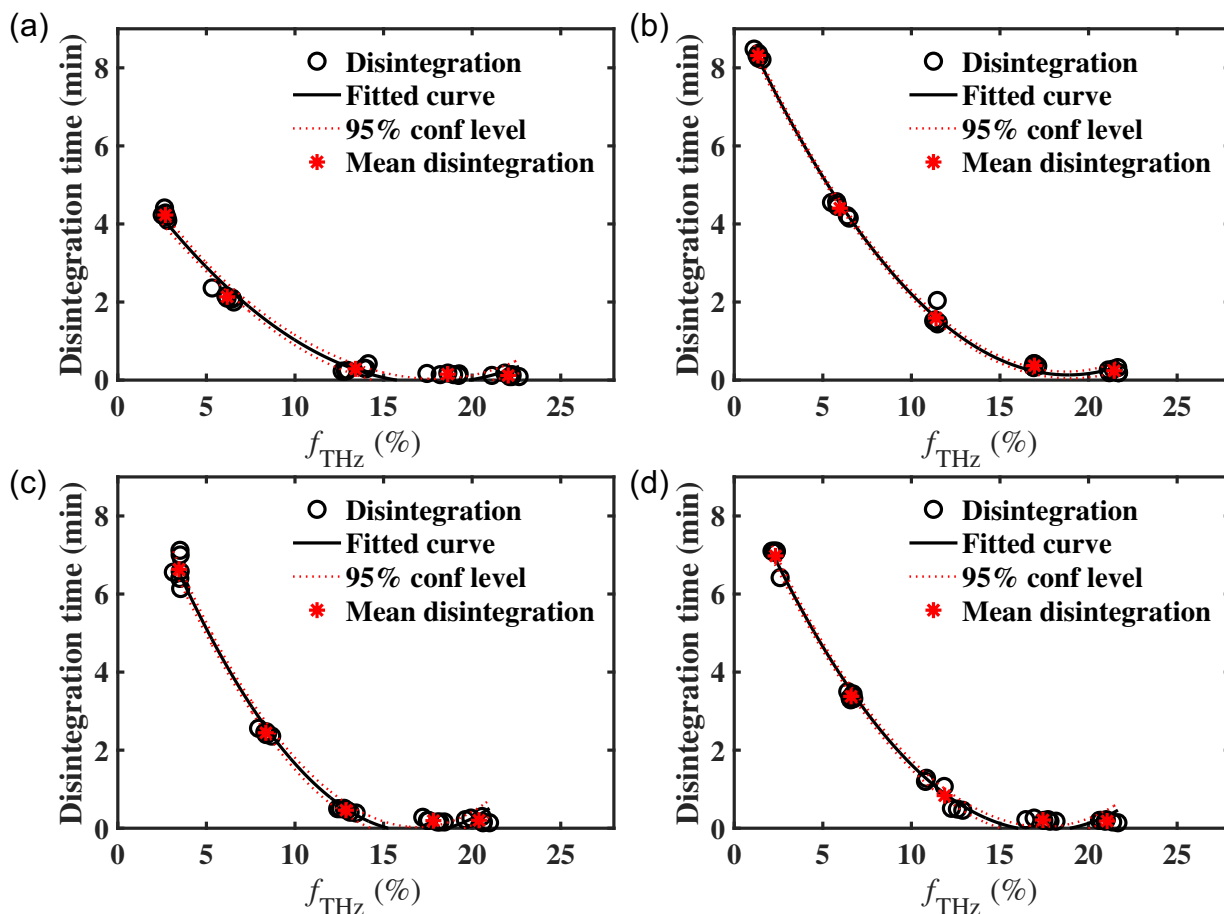


1  
2 **Fig. 3.** The excellent linear correlation between the measured terahertz porosity,  $f_{\text{THz}}$ , and the  
3 nominal porosity,  $f_{\text{nominal}}$ . (a) & (b) represent non-debossed biconvex tablets containing 1%  
4 ibuprofen (F1-Ibup) and 1% indomethacin (F1-Indo) respectively. (c) & (d) are the respective  
5 data for the 10% ibuprofen (F2-Ibup) and 10% indomethacin (F2-Indo) tablets without  
6 debossing, whereas (e) & (f) are the results for the debossed tablets compressed from F2-Ibup  
7 and F2-Indo formulations respectively. The obtained averaged fitting parameters for all batches  
8 are: slope  $\approx 1$ ,  $R^2 \approx 1$  and  $RMSE \approx 0.03\%$ .

### 9 3.3. Correlation between Terahertz Porosity and Disintegration

10 Disintegration testing was performed on biconvex tablets compressed from F1 and F2 API  
11 formulations without debossing (Table 2). A polynomial curve fitting model was used to

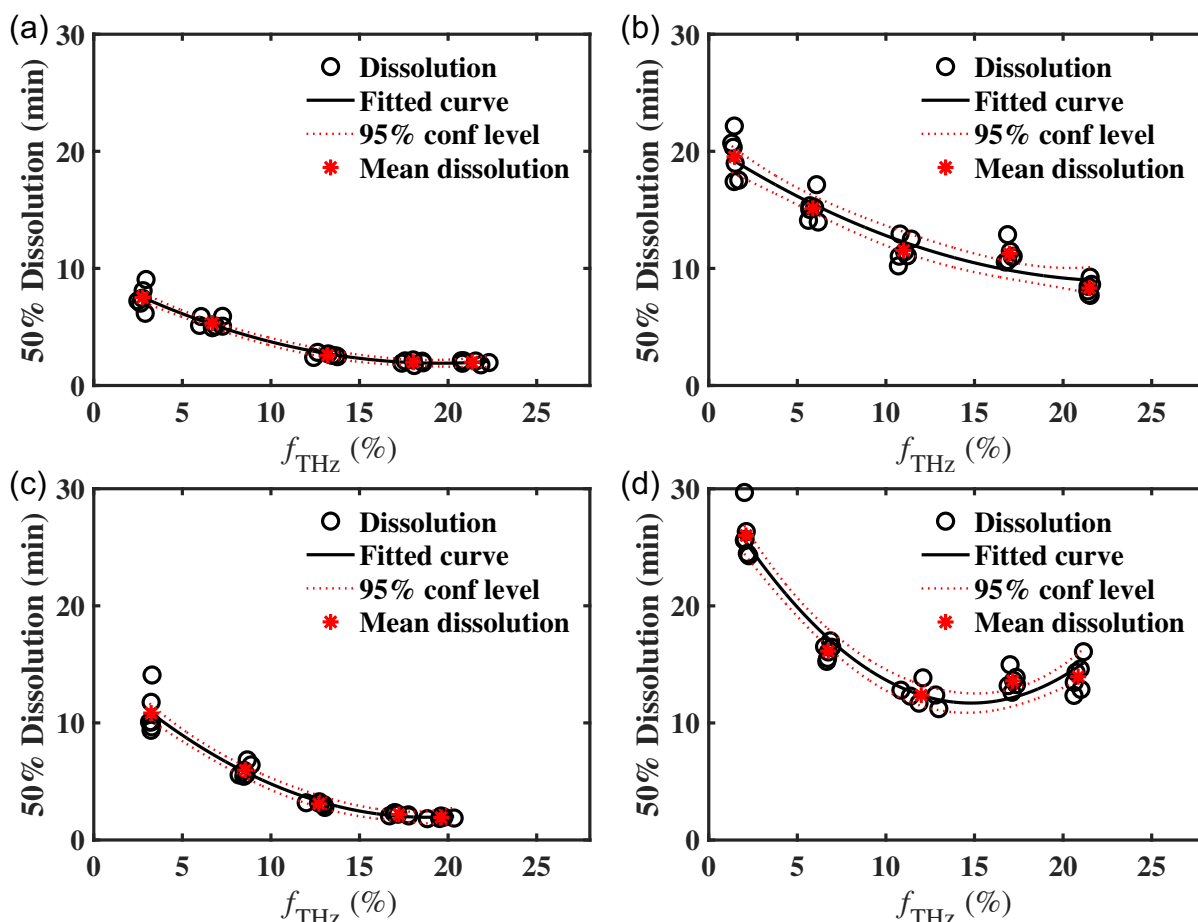
1 correlate the disintegration time with the measured terahertz porosity (Fig. 4). The excellent  
 2 correlations between disintegration time and terahertz porosity manifest the direct influence of  
 3 porosity on tablet disintegration.



4  
 5 **Fig. 4.** The correlation between the disintegration time and the measured terahertz porosity,  
 6  $f_{\text{THZ}}$ . (a) & (b) represent non-debossed biconvex tablets containing 1% ibuprofen (F1-Ibup) and  
 7 1% indomethacin (F1-Indo) respectively. (c) & (d) are the respective data for the 10%  
 8 ibuprofen (F2-Ibup) and 10% indomethacin (F2-Indo) tablets without debossing. Second order  
 9 polynomial data fitting was performed and the averaged fitting parameters that were obtained  
 10 for all sets tablet were  $R^2 \approx 0.99$  and  $RMSE \approx 0.2$  min.

### 11 3.4. Correlation between Terahertz Porosity and Dissolution

12 The dissolution testing was performed on 6 tablets per batch from the same sets used for  
 13 disintegration testing (Table 2). The mean dissolution time at 50% of the drug release of the  
 14 tablets was extracted from the complete dissolution profiles (see Fig. S5 in the supplementary  
 15 information) and plotted against the terahertz porosity (Fig. 5). Aside from the seemingly  
 16 scattering in the data of the indomethacin tablets (Fig. 5 (b) & (c)), a generally good correlation  
 17 can be observed between dissolution time and the measured terahertz porosity. Although  
 18 ibuprofen appears to dissolve faster from the tablets than indomethacin, porosity is again and  
 19 unsurprisingly seen to play a major role in the tablet dissolution kinetics.



1  
2 **Fig. 5.** Correlation between the dissolution time at 50% release of the drug and the terahertz  
3 porosity,  $f_{\text{THz}}$ . (a) & (b) represent biconvex tablets containing 1% ibuprofen and 1%  
4 indomethacin respectively whereas (c) & (d) are the respective data for the 10% ibuprofen and  
5 10% indomethacin tablets without debossing. Second order polynomial data fitting was  
6 performed and the averaged fitting parameters that were obtained for ibuprofen tablets were  $R^2$   
7  $\approx 0.95$  and  $RMSE \approx 0.7$  min, whereas  $R^2 \approx 0.90$  and  $RMSE \approx 1.5$  min were obtained for the  
8 indomethacin tablets.

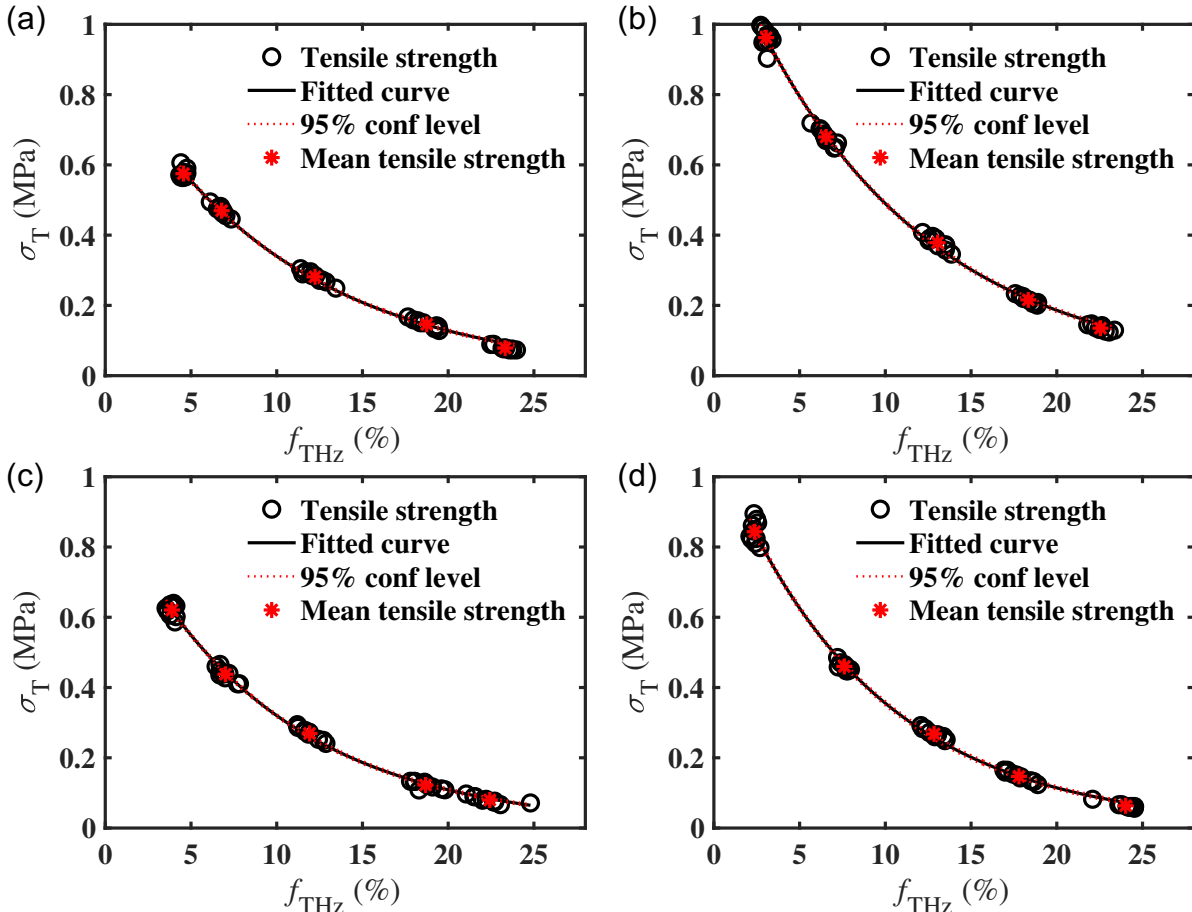
9 Generally, high tablet porosities allow fast liquid penetration/wicking rate, which then quickly  
10 exposes the disintegrant to the penetrating solvent and thus culminating in an increased  
11 swelling rate and the final breakdown of the tablet<sup>22</sup>. However, this is not always the case for  
12 certain types of disintegrants at very high tablet porosity levels (e.g., for rapidly disintegrating  
13 or dissolving tablets). The swelling of disintegrant like CCS has been reported to be  
14 accompanied by gel formation that can significantly prolong the disintegration time<sup>26</sup>. The  
15 presence of gel can occlude the pores and hence delay the liquid uptake rate. A similar  
16 phenomenon is observed in this study (see Fig. 5(d)), which explains our choice to use a  
17 polynomial regression method. The polynomial equation is used strictly as a regression method  
18 and is not thought to afford further physical insight, but it can capture a minimum in dissolution  
19 time over the experimental porosity range, to determine the relation between  
20 dissolution/disintegration and porosity (see Figs. 4 and 5). In as much as the current analyses  
21 place much emphases on the influence of porosity, we are very much aware of the significant  
22 role played by other factors such as hydrophilicity (contact angle), wetting time and water

1 absorption ratio on the dissolution/disintegration time of especially orodispersible tablets (ODTs)  
2 26,47,48.

3 It should be clarified at this point that, although the dissolution behaviour of a given drug  
4 substance significantly depends on its solubility properties, the rate at which the tablet  
5 disintegrates also plays a significant role by exposing the drug particles to the dissolution  
6 medium. The relative short disintegration times of the ibuprofen tablets compared to that of the  
7 indomethacin tablets (see Fig. 4) partly explains the trend in dissolution rates of ibuprofen and  
8 indomethacin observed in Fig. 5. Other contributing factors to the observed dissolution  
9 behaviours of the two APIs may include material attribute like particle size distribution and the  
10 different PH values of the dissolution media.

### 11 3.5. Correlation between Terahertz Porosity and Tensile Strength

12 Despite our previous study that has revealed that hardness does not always correlate with the  
13 porosity (especially for granulated samples) <sup>17</sup>, the current samples have shown excellent  
14 correlation between the tensile strength and terahertz-based porosity values (Fig. 6). The  
15 samples used in this study were directly compressed without any upstream processing of the  
16 powder blends (e.g. granulation).



17  
18 **Fig. 6.** The correlation between the tensile strength,  $\sigma_T$ , and the measured terahertz porosity,  
19  $f_{THz}$ . (a) & (b) represent non-debossed biconvex tablets containing 1% ibuprofen (F1-Ibup) and  
20 1% indomethacin (F1-Indo) respectively. (c) & (d) are the respective data for the 10%  
21 ibuprofen (F2-Ibup) and 10% indomethacin (F2-Indo) tablets without debossing. The averaged  
22 fitting parameters that were obtained using the Ryshkewitch-Duckworth Equation <sup>49-51</sup> of all  
23 sets of tablet were  $R^2 \approx 0.99$  and  $RMSE \approx 0.014$  MPa.

1 To summarise the above results, it is observed that the ibuprofen-based tablets tend to  
2 disintegrate and dissolve faster than the indomethacin tablets, which is unsurprisingly  
3 consistent with their respective tensile strength data. The seemingly scattering observed in  
4 some of the results may have been emanated from experimental inconsistencies. For example,  
5 during the disintegration testing, there were occasions when a disk got stuck on a tablet  
6 restricting the movement of the tablet during the up and down strokes. Such situations cause a  
7 delay in the overall disintegration time of that particular tablet due to limited exposure of the  
8 concerned tablet to the immersion liquid. Finally, the use of a simple polynomial curve fitting  
9 described the relationship between the porosity and the disintegration time as well as  
10 dissolution data well for all the tested batches tablets.

#### 11 **4. Conclusions**

12 This study demonstrated the robustness of a fast and non-destructive terahertz porosity  
13 measurement method that can predict drug release properties (disintegration time and  
14 dissolution) of pharmaceutical tablets. By using THz-TDS, the porosity of different kinds of  
15 tablets was directly measured in a fast manner ( $\leq 1$  s). The various kinds of tablets used were  
16 composed of either ibuprofen or indomethacin under two dose strengths, 1% and 10%. All the  
17 tablets were formulated with commonly used excipients (microcrystalline cellulose, lactose  
18 anhydrous, croscarmellose sodium, and magnesium stearate).

19 The excellent linear correlation observed between the terahertz porosity and the nominal  
20 porosity has manifested the robustness of the terahertz approach for tablet porosity  
21 measurement even for tablets containing high absorbing APIs, embossing and of different  
22 geometries. Moreover, the observed promising correlations of the terahertz porosity with  
23 dissolution, disintegration and hardness/tensile strength demonstrate the ability of using the  
24 terahertz porosity method for RTRT of tablet dissolution.

25 Despite the non-destructive nature of the THz method, it still faces some challenges given the  
26 use of porosity as the only parameter to predict the release and dissolution properties of a drug  
27 from tablets. Hence this method is suitable for rapidly disintegration tablets containing highly  
28 soluble APIs. Future studies with the aim of developing a universal method should consider  
29 other properties like swelling and liquid ingress mechanisms<sup>48</sup>, the pore shape and structure<sup>16</sup>  
30 as well as the solubility and dissolution properties of the API. A detailed discussion on the  
31 terahertz porosity method has been highlighted in recent review by Lu et al<sup>52</sup>.

#### 32 **Acknowledgements**

33 The research received financial support from Innovate UK (ref: 104196).

#### 34 **REFERENCES**

- 35 1. Industry G for. Guidance for Industry PAT — A Framework for Innovative  
36 Pharmaceutical Development, Manufacturing, and Quality Assurance. *FDA Off Doc.*  
37 2004;(September):16. doi:http://www.fda.gov/CDER/guidance/6419fnl.pdf
- 38 2. Schlindwein WS, Gibson M. *Pharmaceutical Quality by Design: A Practical*  
39 *Approach.*; 2017. doi:10.1002/9781118895238
- 40 3. European Medicines Agency. Guideline on Real Time Release Testing  
41 EMA/CHMP/QWP/811210/2009-Rev1. *Comm Med Prod Hum Use.*

- 1 2012;44(March):1-10. [https://www.ema.europa.eu/en/documents/scientific-](https://www.ema.europa.eu/en/documents/scientific-guideline/guideline-real-time-release-testing-formerly-guideline-parametric-release-revision-1_en.pdf)  
2 [guideline/guideline-real-time-release-testing-formerly-guideline-parametric-release-](https://www.ema.europa.eu/en/documents/scientific-guideline/guideline-real-time-release-testing-formerly-guideline-parametric-release-revision-1_en.pdf)  
3 [revision-1\\_en.pdf](https://www.ema.europa.eu/en/documents/scientific-guideline/guideline-real-time-release-testing-formerly-guideline-parametric-release-revision-1_en.pdf). Accessed October 12, 2019.
- 4 4. Markl D, Warman M, Dumarey M, et al. Review of Real-Time Release Testing of  
5 Pharmaceutical Tablets: State-of-the Art, Challenges and Future Perspective. *Int J*  
6 *Pharm.* April 2020;119353. doi:10.1016/j.ijpharm.2020.119353
- 7 5. Pawar P, Wang Y, Keyvan G, Callegari G, Cuitino A, Muzzio F. Enabling real time  
8 release testing by NIR prediction of dissolution of tablets made by continuous direct  
9 compression (CDC). *Int J Pharm.* 2016;512(1):96-107.  
10 doi:10.1016/j.ijpharm.2016.08.033
- 11 6. Hernandez E, Pawar P, Keyvan G, et al. Prediction of dissolution profiles by non-  
12 destructive near infrared spectroscopy in tablets subjected to different levels of strain.  
13 *J Pharm Biomed Anal.* 2016;117:568-576. doi:10.1016/j.jpba.2015.10.012
- 14 7. Shah RB, Tawakkul MA, Khan MA. Process analytical technology: Chemometric  
15 analysis of raman and near infra-red spectroscopic data for predicting physical  
16 properties of extended release matrix tablets. *J Pharm Sci.* 2007;96(5):1356-1365.  
17 doi:10.1002/jps.20931
- 18 8. Freitas MP, Sabadin A, Silva LM, et al. Prediction of drug dissolution profiles from  
19 tablets using NIR diffuse reflectance spectroscopy: A rapid and nondestructive  
20 method. *J Pharm Biomed Anal.* 2005;39(1-2):17-21. doi:10.1016/j.jpba.2005.03.023
- 21 9. Yekpe K, Abatzoglou N, Bataille B, et al. Predicting the dissolution behavior of  
22 pharmaceutical tablets with NIR chemical imaging. *Int J Pharm.* 2015;486(1-2):242-  
23 251. doi:10.1016/j.ijpharm.2015.03.060
- 24 10. Nott KP. Magnetic resonance imaging of tablet dissolution. *Eur J Pharm Biopharm.*  
25 2010;74(1):78-83. doi:10.1016/j.ejpb.2009.07.003
- 26 11. Mikac U, Demsar A, Demsar F, Serša I. A study of tablet dissolution by magnetic  
27 resonance electric current density imaging. *J Magn Reson.* 2007;185(1):103-109.  
28 doi:10.1016/j.jmr.2006.12.002
- 29 12. Dumarey M, Goodwin DJ, Davison C. Multivariate modelling to study the effect of  
30 the manufacturing process on the complete tablet dissolution profile. *Int J Pharm.*  
31 2015;486(1-2):112-120. doi:10.1016/j.ijpharm.2015.03.040
- 32 13. Kimber JA, Kazarian SG, Štěpánek F. Microstructure-based mathematical modelling  
33 and spectroscopic imaging of tablet dissolution. *Comput Chem Eng.* 2011;35(7):1328-  
34 1339. doi:10.1016/j.compchemeng.2010.07.008
- 35 14. Kimber JA, Kazarian SG, Štěpánek F. Modelling of pharmaceutical tablet swelling  
36 and dissolution using discrete element method. *Chem Eng Sci.* 2012;69(1):394-403.  
37 doi:10.1016/j.ces.2011.10.066
- 38 15. Nagy B, Petra D, Galata DL, et al. Application of artificial neural networks for Process  
39 Analytical Technology-based dissolution testing. *Int J Pharm.* 2019;567(March).  
40 doi:10.1016/j.ijpharm.2019.118464
- 41 16. Markl D, Strobel A, Schlossnikl R, et al. Characterisation of Pore Structures of  
42 Pharmaceutical Tablets: A Review. *Int J Pharm.* 2018;538(1-2):188-214.  
43 doi:https://doi.org/10.1016/j.ijpharm.2018.01.017
- 44 17. Markl D, Sauerwein J, Goodwin DJ, Van Den Ban S, Zeitler JA, Zeitler & JA. Non-  
45 destructive Determination of Disintegration Time and Dissolution in Immediate  
46 Release Tablets by Terahertz Transmission Measurements. *Pharm Res.*  
47 2017;34(5):1012-1022. doi:10.1007/s11095-017-2108-4
- 48 18. ICH Harmonised Tripartite Guideline, Q6A Specifications: Test Procedures and  
49 Acceptance Criteria for New Drug Substances and New Drug Products: Chemical  
50 Substances | FDA. <https://www.fda.gov/regulatory-information/search-fda-guidance->

- 1 documents/q6a-specifications-test-procedures-and-acceptance-criteria-new-drug-  
2 substances-and-new-drug-products. Published 1999. Accessed October 19, 2019.
- 3 19. Nickerson B, Kong A, Gerst P, Kao S. Correlation of dissolution and disintegration  
4 results for an immediate-release tablet. *J Pharm Biomed Anal.* 2018;150:333-340.  
5 doi:10.1016/j.jpba.2017.12.017
- 6 20. Grube A, Gerlitzki C, Brendel M. Dissolution or disintegration–substitution of  
7 dissolution by disintegration testing for a fixed dose combination product. *Drug Dev*  
8 *Ind Pharm.* 2019;45(1):130-138. doi:10.1080/03639045.2018.1526184
- 9 21. Wilson D, Wren S, Reynolds G. Linking dissolution to disintegration in immediate  
10 release tablets using image analysis and a population balance modelling approach.  
11 *Pharm Res.* 2012;29(1):198-208. doi:10.1007/s11095-011-0535-1
- 12 22. Markl D, Zeitler JA. A Review of Disintegration Mechanisms and Measurement  
13 Techniques. *Pharm Res.* 2017;34(5):890-917. doi:10.1007/s11095-017-2129-z
- 14 23. Shah U, Augsburger L. Evaluation of the functional equivalence of crospovidone NF  
15 from different sources. I. Physical characterization. *Pharm Dev Technol.* 2001;6(1):39-  
16 51. doi:10.1081/PDT-100000012
- 17 24. Desai PM, Liew CV, Heng PWS. Review of Disintegrants and the Disintegration  
18 Phenomena. *J Pharm Sci.* 2016;105(9):2545-2555. doi:10.1016/J.XPHS.2015.12.019
- 19 25. Yassin S, Su K, Lin H, Gladden LF, Zeitler JA. Diffusion and swelling measurements  
20 in pharmaceutical powder compacts using terahertz pulsed imaging. *J Pharm Sci.*  
21 2015;104(5):1658-1667. doi:10.1002/jps.24376
- 22 26. Bi YX, Sunada H, Yonezawa Y, Danjo K. Evaluation of rapidly disintegrating tablets  
23 prepared by a direct compression method. *Drug Dev Ind Pharm.* 1999;25(5):571-581.  
24 doi:10.1081/DDC-100102211
- 25 27. Hattori Y, Otsuka M. NIR spectroscopic study of the dissolution process in  
26 pharmaceutical tablets. *Vib Spectrosc.* 2011;57(2):275-281.  
27 doi:10.1016/j.vibspec.2011.09.003
- 28 28. Delalonde M, Ruiz T. Dissolution of pharmaceutical tablets: The influence of  
29 penetration and drainage of interstitial fluids. *Chem Eng Process Process Intensif.*  
30 2008;47(3):370-376. doi:10.1016/j.cep.2007.01.003
- 31 29. Riippi M, Yliruusi J, Niskanen T, Kiesvaara J. Dependence between dissolution rate  
32 and porosity of compressed erythromycin acistrate tablets. *Eur J Pharm Biopharm.*  
33 1998;46(2):169-175. doi:10.1016/S0939-6411(98)00003-4
- 34 30. Ridgway C, Bawuah P, Markl D, et al. On the role of API in determining porosity,  
35 pore structure and bulk modulus of the skeletal material in pharmaceutical tablets  
36 formed with MCC excipient. *Int J Pharm.* 2017;526(1):321-331.  
37 doi:10.1016/j.ijpharm.2017.04.038
- 38 31. Markl D, Wang P, Ridgway C, et al. Characterization of the Pore Structure of  
39 Functionalized Calcium Carbonate Tablets by Terahertz Time-Domain Spectroscopy  
40 and X-Ray Computed Microtomography. *Journal of Pharmaceutical Sciences.*  
41 <http://www.sciencedirect.com/science/article/pii/S0022354917301430>. Published  
42 2017. Accessed July 5, 2017.
- 43 32. Bawuah P, Pierotic Mendia A, Silfsten P, et al. Detection of porosity of  
44 pharmaceutical compacts by terahertz radiation transmission and light reflection  
45 measurement techniques. *Int J Pharm.* 2014;465(1-2):70–76.  
46 doi:10.1016/j.ijpharm.2014.02.011
- 47 33. Bawuah P, Ervasti T, Tan N, Zeitler JA, Ketolainen J, Peiponen K-E. Noninvasive  
48 porosity measurement of biconvex tablets using terahertz pulses. *Int J Pharm.*  
49 2016;509(1-2):439-443. doi:10.1016/J.IJPHARM.2016.06.023
- 50 34. Bawuah P, Markl D, Farrell D, et al. Terahertz-Based Porosity Measurement of

- 1 Pharmaceutical Tablets: a Tutorial. *J Infrared, Millimeter, Terahertz Waves*. January  
2 2020;1-20. doi:10.1007/s10762-019-00659-0
- 3 35. Jepsen PU. Phase Retrieval in Terahertz Time-Domain Measurements: a “how to”  
4 Tutorial. *J Infrared, Millimeter, Terahertz Waves*. 2019;40(4):395-411.  
5 doi:10.1007/s10762-019-00578-0
- 6 36. Dorney TD, Baraniuk RG, Mittleman DM. Material parameter estimation with  
7 terahertz time-domain spectroscopy. *J Opt Soc Am A-Opt Image Sci Vis*.  
8 2001;18(7):1562-1571. doi:10.1364/JOSAA.18.001562
- 9 37. Jepsen PU, Cooke DG, Koch M. Terahertz spectroscopy and imaging - Modern  
10 techniques and applications. *Laser Photon Rev*. 2011;5(1):124-166.  
11 doi:10.1002/lpor.201000011
- 12 38. Withayachumnankul W, Naftaly M. Fundamentals of Measurement in Terahertz Time-  
13 Domain Spectroscopy. *J Infrared, Millimeter, Terahertz Waves*. 2014;35(8):610-637.  
14 doi:10.1007/s10762-013-0042-z
- 15 39. Scheller M. Data Extraction from Terahertz Time Domain Spectroscopy  
16 Measurements. *J Infrared, Millimeter, Terahertz Waves*. 2014;35(8):638-648.  
17 doi:10.1007/s10762-014-0053-4
- 18 40. Singh SP, Akhter Z, Akhtar MJ. Calibration Independent Estimation of Optical  
19 Constants Using Terahertz Time-Domain Spectroscopy. *Microw Opt Technol Lett*.  
20 2015;57(8):1861-1864. doi:10.1002/mop
- 21 41. United States Pharmacopeia. Disintegration.  
22 [https://www.usp.org/sites/default/files/usp/document/harmonization/gen-chapter/april-](https://www.usp.org/sites/default/files/usp/document/harmonization/gen-chapter/april-2019-m99460.pdf)  
23 [2019-m99460.pdf](https://www.usp.org/sites/default/files/usp/document/harmonization/gen-chapter/april-2019-m99460.pdf). Accessed February 9, 2020.
- 24 42. European Pharmacopoeia 5.0. Pharmaceutical technical procedures.  
25 <http://uspbpep.com/ep50/2.9.1.disintegration.of.tablets.and.capsules.pdf>. Accessed  
26 February 9, 2020.
- 27 43. British Pharmacopoeia Commission. British Pharmacopoeia 2020: Volume III -  
28 Formulated Preparations: Specific Monographs. 2020.  
29 <https://www.pharmacopoeia.com/downloads/bp/2020/>. Accessed February 26, 2020.
- 30 44. United States Pharmacopoeia 2017. Revision Bulletin. 2017. <https://www.usp.org/>.  
31 Accessed February 26, 2020.
- 32 45. Pitt KG, Heasley MG. Determination of the tensile strength of elongated tablets.  
33 *Powder Technol*. 2013;238:169-175. doi:10.1016/j.powtec.2011.12.060
- 34 46. Pitt KG, Newton JM, Stanley P. Tensile fracture of doubly-convex cylindrical discs  
35 under diametral loading. *J Mater Sci*. 1988;23(8):2723-2728.  
36 doi:10.1007/BF00547442
- 37 47. Pabari RM, Ramtoola Z. Effect of a disintegration mechanism on wetting, water  
38 absorption, and disintegration time of orodispersible tablets. *J Young Pharm*.  
39 2012;4(3):157-163. doi:10.4103/0975-1483.100021
- 40 48. Al-Sharabi M, Markl D, Mudley T, et al. Simultaneous investigation of the liquid  
41 transport and swelling performance during tablet disintegration. *Int J Pharm*.  
42 2020;584. doi:10.1016/j.ijpharm.2020.119380
- 43 49. Wu CY, Best SM, Bentham AC, Hancock BC, Bonfield W. A simple predictive model  
44 for the tensile strength of binary tablets. *Eur J Pharm Sci*. 2005;25(2-3):331-336.  
45 doi:10.1016/j.ejps.2005.03.004
- 46 50. Duckworth, W. Discussion of Ryshkewitch Paper by Winston Duckworth. *J Am*  
47 *Ceram Soc*. 1953;36(2):68-68. doi:10.1111/j.1151-2916.1953.tb12838.x
- 48 51. Ryshkewitch E. Compression Strength of Porous Sintered Alumina and Zirconia: 9th  
49 Communication to Ceramography. *J Am Ceram Soc*. 1953;36(2):65-68.  
50 doi:10.1111/j.1151-2916.1953.tb12837.x

- 1 52. Lu X, Sun H, Chang T, Zhang J, Cui HL. Terahertz detection of porosity and porous  
2 microstructure in pharmaceutical tablets: A review. *Int J Pharm.* 2020;591:378-5173.  
3 doi:10.1016/j.ijpharm.2020.120006  
4  
5